Membrane-associated Lamins in Xenopus Egg Extracts: Identification of Two Vesicle Populations

David Lourim and Georg Krohne

Division of Electron Microscopy, Theodor Boveri Institute, University of Würzburg, Am Hubland, D-97074 Würzburg, Germany

Abstract. Nuclear lamin isoforms of vertebrates can be divided into two major classes. The B-type lamins are membrane associated throughout the cell cycle, whereas A-type lamins are recovered from mitotic cell homogenates in membrane-free fractions. A feature of oogenesis in birds and mammals is the nearly exclusive presence of B-type lamins in oocyte nuclear envelopes. In contrast, oocytes and early cleavage embryos of the amphibian *Xenopus laevis* are believed to contain a single lamin isoform, lamin L_{III}, which after nuclear envelope breakdown during meiotic maturation is reported to be completely soluble. Consequently, we have reexamined the lamin complement of *Xenopus* oocyte nuclear envelopes, egg extracts, and early embryos. An mAb (X223) specific for the homologous B-type lamins B_2 of mouse and L_{II} of *Xenopus* somatic cells (Höger, T., K. Zatloukal, I. Waizenegger, and G. Krohne. 1990. *Chromosoma.* 99:379–390) recognized a *Xenopus* oocyte nuclear envelope protein biochemically distinct from lamin L_{III} and very similar or identical to somatic cell lamin L_{II}. Oocyte lamin L_{II} was detectable in nuclear envelopes of early cleavage embryos. Immunoblotting of fractionated egg extracts revealed that ~20–23% of lamin L_{II} and 5–7% of lamin L_{III} were membrane associated. EM immunolocalization demonstrated that membrane-bound lamins L_{II} and L_{III} are associated with separate vesicle populations. These findings are relevant to the interpretation of nuclear reconstitution experiments using *Xenopus* egg extracts.

THE quantitatively major proteins of the nuclear envelope lamina, the nuclear lamins, are members of the multigene family of intermediate filament proteins (11, 16, 23, 33, 39, 44, 54). It has been suggested that lamins may be involved in the regulation of chromatin topology (2, 4, 6, 15, 18, 28, 32) and indirectly involved in DNA replication (19, 34, 36), differential gene expression (31, 32), and nuclear envelope re-formation after mitosis (6, 47) as well as meiosis (10).

Two major lamin isotypes can be distinguished according to their biochemistry in mitotic and meiotic cells. B-type lamins remain associated with membranes, whereas A-type lamins depolymerize into distinct soluble oligomers not in contact with membranes (6, 13, 46; for comparison of amino acid sequences see references 16, 23, 39). A- and B-type lamins further differ in their posttranslational proteolytic processing at the carboxy terminus (3, 50, 51).

The expression of A- and B-type lamin isoforms in vertebrates is developmentally regulated in a tissue-specific manner (for reviews see references 20, 37). Chicken (29) and mouse oocytes (41, 42) appear to contain both A- and B-type lamins. However, A-type lamins quickly disappeared from early embryos of both species, and later became increasingly prominent in a developmentally regulated, tissue-specific manner (27, 29, 30, 40, 42).

In contrast to the situation in mouse and chicken oocyte nuclear envelopes, the amphibian *Xenopus laevis* oogenic cells, eggs, and early embryos are believed to contain a single lamin isoform, lamin L_{III}, which, after nuclear envelope breakdown during meiotic maturation of eggs, is reported to be quantitatively soluble in a form sedimenting at 8–9 S (5, 21, 36). cDNA sequencing had identified two alternatively spliced lamin L_{III} mRNAs differing by 12 amino acids at the direct carboxy terminus, neither of which conveniently classifies as A- or B-type lamins because they possess amino acid sequence similarities to each (11, 43). It has been proposed that lamin L_{III} proteins and transcripts serve as a maternally derived pool for the formation of pronuclei and early cleavage nuclei (43, 45). During development, lamin L_{III} has reportedly been replaced in embryonic nuclei by the B-type lamins L_I and L_{II} at the midblastula and gastrula stages, respectively. Later, lamin L_{III} was reexpressed in a few types of differentiated cells of adult tissues (5). A-type lamin expression was first detected in the swimming tadpole (53).

Based on the generally conserved, developmentally regulated, and tissue-specific patterns of A- and B-type lamin expression across vertebrate species, it is surprising that one or more B-type lamin isoforms have not yet been detected in *Xenopus* oocyte or early embryonic nuclei. The increasing use of *Xenopus* egg cell-free systems to analyze the function of nuclear proteins (for reviews see references 8, 26) has prompted us to reexamine the lamin complement of *Xenopus* oocytes, egg extracts, and early embryos.

Using antinuclear lamin isoform-specific antibodies, we have demonstrated that oocytes, egg extracts, and early embryos contain a B-type lamin in addition to lamin L_{III}. This B-type lamin is biochemically similar if not identical to lamin L_{II} of somatic cells. Using ultracentrifugation and EM techniques, we have identified lamin L_{II}-associated vesicles in meiotic egg extracts. Unexpectedly, a small percentage of lamin L_{III} was also associated with vesicles in egg extracts. Our description of lamin-associated vesicles in *Xenopus* egg extracts may help to resolve contradictory suggestions regarding lamin function in targeting vesicles to chromatin during nuclear envelope reassembly.

Materials and Methods

Animals and Embryos

Adult female and male *X. laevis* were obtained from the South African Snake Farm (Fish Hoek, South Africa). Embryos were reared from eggs that had been fertilized in vitro (5).

Antibodies

The mAbs $L_0$46F7 (hereafter referred to as 46F7) and X223 have been described previously (5, 16). The mAbs recognizing lamins L_{II} and L_{III} (X155) and lamins A and L_I (X67) were produced and characterized as described (16, 17). The broad-reacting antilamin mAb PKB8 has been described previously (22). The guinea pig antiserum against the nuclear envelope pore complex protein, gp62, has been described previously (7). Polyclonal rabbit antibodies against the chicken transmembrane protein p54, which localize to the inner nuclear membrane (1) and cross-react with the homologous protein of *Xenopus*, were kindly provided by Dr. Erich Nigg (Swiss Institute for Experimental Cancer Research, Epalinges, Switzerland).

Preparation of Xenopus Oocyte and Egg Fractions

Oocyte nuclear envelopes and cytoplasmic supernatants were prepared from manually isolated and defolliculated mature oocytes. All procedures and buffers were at 4°C. Briefly, follicle cells and germinal vesicles were manually isolated from mature oocytes in 5:1 medium (83 mM KCl, 17 mM NaCl, 6.5 mM Na_2HPO_4, 3.5 mM NaH_2PO_4) and incubated for 10 min on ice in 5:1 medium/1 M NaCl (salt wash) before concentration by centrifugation at 10,000 *g* for 10 min. For Triton X-100 extraction of nuclear envelopes, salt-washed oocyte nuclei were incubated in 5:1 medium/2% Triton X-100 for 10 min on ice, then centrifuged at 5,000 *g* in a tabletop centrifuge; the extraction was repeated, and nuclei were pelleted by centrifugation at 10,000 *g*. The supernatants were combined and the samples analyzed by Western blotting of an equal percentage of the Triton pellet and supernatant.

High-speed centrifugation fractions of meiotic egg extracts were prepared from unactivated *Xenopus* eggs. All procedures and buffers were at 4°C. Briefly, eggs dejellied with 2% L-cysteine (pH 7.8) were washed three times with MEB buffer (50 mM KCl, 20 mM β-glycerophosphate, 2 mM $MgCl_2$, 1 mM DTT, 1 mM EGTA, 5 μg/ml cytochlasin B, 1 mM ATP, 10 μM GTPγS, 1 mM PMSF, 10 μg/ml aprotinin and leupeptin, 10 mM Hepes, pH 7.5) containing 250 mM sucrose. Approximately 1 ml per Eppendorf tube of packed eggs was crushed by centrifugation for 10 min at 10,000 *g* in a tabletop centrifuge, then the cloudy cytoplasm was removed and centrifuged for 20 min at 10,000 rpm in an ultracentrifuge (model L7-80; Beckman Instruments, Inc., Palo Alto, CA) with an SW50.1 rotor. The cleared supernatant was then centrifuged at 35,000 rpm (100,000 *g*, SW50.1 rotor) for 60 min to generate the S_{100} supernatant (S_{100} Sup.), and the pellet, which contained a majority of the mitochondria and did not contain detectable amounts of lamins, was discarded. Membranes were collected from the S_{100} Sup. by a sixfold dilution with MEB and centrifuged at 200,000 *g* for 2 h. The supernatant (S_{200} Cytosol) was shock frozen in liquid nitrogen and stored at −70°C. The membrane-enriched pellet (S_{200} Pellet) was washed by resuspension in MEB containing 250 mM sucrose, overlayed onto five volumes of MEB/250 mM sucrose, and centrifuged at 20,000 rpm for 20 min in the SW50.1 rotor. Final membrane pellets were resuspended in MEB/500 mM sucrose at 1/10 the original volume of S_{100} Sup. before shock freezing in liquid nitrogen. To assay for membranes in the S_{200} Cytosol, an equal volume of a fixation buffer (2.5% gluteraldehyde, 50 mM KCl, 2.5 mM $MgCl_2$, 50 mM cacodylate, pH 7.2) was added to the cytosol and centrifuged at 10,000 *g* for 45 min. The pellet was postfixed with osmium tetroxide and uranyl acetate, then embedded in Epon 812 for thin section EM analysis as previously described (14).

Immunoabsorption of Membranes from Mitotic Egg Fractions

Membranes were immunologically isolated from freshly prepared S_{100} Sup. using goat anti-mouse antibody-coupled magnetic beads (IO beads; Dianova, Hamburg, Germany) to which the primary monoclonal antilamin antibodies 46F7 or X223 had been coupled essentially as recommended by the manufacturer. 100 μl of S_{100} Sup. was made to 1 ml with MEB buffer/250 mM sucrose for incubation with the antibody-coated magnetic beads. All samples were preabsorbed for 30 min at 4°C with 30 μl (original volume) goat anti-mouse antibody-coupled beads. Immunoabsorptions with 5–40 μl (original volume) primary antibody-coated beads were carried out overnight at 4°C with gentle rocking. Isolation of the magnetic beads was essentially performed as recommended by the manufacturer. However, because of the high viscosity of the samples, it was necessary to increase the recommended times of bead absorption to the magnet. Immunobeads were washed with 2 ml MEB/250 mM sucrose three times before freezing for biochemical analysis, or immediately processed for embedding and ultrastructural analysis by standard fixation and staining protocols and embedding in Epon 812 (14).

Immunofluorescence

For immunofluorescence microscopy on frozen sections through *Xenopus* ovary, immunostaining was performed essentially as described by Krohne et al. (22). Primary antibodies were diluted 1:1,000 and visualized with goat anti-mouse secondary antibodies conjugated to Texas red (Dianova) diluted 1:150. For visualization of chromatin, preparations were stained with HOECHST 33258 (2.5 μg/ml) simultaneously with the second antibody.

For immunofluorescence analysis of early embryos, embryos obtained from in vitro fertilized eggs (5) were dejellied, and then cultured at room temperature in 5% MMR (100 mM NaCl, 2 mM KCl, 1 mM $MgSO_4$, 0.1 mM EDTA, 5 mM Hepes, pH 7.8) for various numbers of cell divisions before transfer into 5% MMR containing 0.4 mg/ml cycloheximide for 1 h to arrest cells in interphase. Staged embryos were squashed between glass slides and coverslips and frozen by application to dry ice. Coverslips were removed from the slides while frozen and the specimens air dried for 30–60 min before extraction with cold acetone for 10 min. Squashed preparations were then analyzed by immunofluorescence as described for frozen sections. Photographs were taken with a microscope (Axiophot; Zeiss, Oberkochen, Germany) equipped with epifluorescence optics and appropriate filter sets.

Immunoelectron Microscopy

Nuclear envelopes isolated from mature oocytes were incubated first with the mAb X223, then with goat anti-mouse antibodies conjugated to 10-nm gold particles (Dianova) essentially as described (5).

For immunolocalization of lamins in meiotic egg membranes, aliquots of the S_{200} pellet fraction in MEB buffer were centrifuged at 3,000 *g* for 5 min at 4°C (Minifuge RF; Heraeus; Osterode, Germany) onto 0.1 μg/ml poly-L-lysine hydrobromide (Sigma Chemical GmbH, Munich, Germany)-coated coverslips (10-min incubation and then air dried). After washing to remove nonadherent materials, the coverslips were incubated with ascites fluid of the antibodies 46F7 or X223 diluted 1:200 in MEB (minus DTT), or as a control in MEB (minus DTT) alone, for 1 h at room temperature in a humidified chamber. After three 5-min washes with MEB buffer (minus DTT) containing 0.1% BSA, the membranes were incubated with 12-nm gold-conjugated goat anti-mouse antibodies (Dianova) in the wash buffer for 60 min. The membranes were washed as indicated above, then fixed and embedded as described (14). Ultrathin sections were stained according to standard protocols and examined in an electron microscope (EM 10; Zeiss) at 80 kV.

Gel Electrophoresis and Immunoblotting

One-dimensional gel electrophoresis was performed with 8 or 11% SDS-PAGE gels essentially as described by Laemmli (25). NEPHGE was

based on a modification of the method of O'Farrell et al. (38) and included pH 3.5–10 Ampholines (3%) and pH 5–8 ampholines (2%; Pharamacia, Freiburg, Germany) in the first-dimension gel mixture. 11% SDS-PAGE gels were used for the separation in the second dimension. Isoelectric point standards skeletal α-actin (5 μg), phosphoglucose kinase (5 μg), and BSA (2 μg) were added to samples before first-dimension electrophoresis.

After one- or two-dimensional gel separation, proteins were electrophoretically transferred to nitrocellulose filters (Schleicher & Schuell, Dassel, Germany) using the semidry method (24) in a graphite chamber (Hartenstein, Würzburg, Germany). Nitrocellulose filters were stained with Ponceau S to mark the position of protein standards, then blocked overnight at 4°C in 5% nonfat dry milk in TBST[1] (140 mM NaCl, 0.3% Tween, 10 mM Tris, pH 8.0). Filters were incubated for 1 h at room temperature with primary antibodies diluted 1:1,000 in TBST plus 5% nonfat dry milk (except X223, which was diluted in TBST alone). The filters were washed 3 times for 10 min in TBST plus 0.1% Triton X-100, then twice for 5 min in TBST. The filters were then incubated for 1 h at room temperature in appropriate species-specific HRP-conjugated secondary antibodies (Jackson Immuno-Research Laboratories, Inc., West Grove, PA) diluted 1:10,000 in TBST plus 5% nonfat dry milk. After washing as outlined above, the positions of bound antibodies were detected using the enhanced chemiluminescence system (Amersham Buchler GmBH, Braunschweig, Germany) by exposure to film (X-Omat AR; Eastman Kodak Co., Rochester, NY).

Results

Characterization of Oocyte Nuclear Envelope Lamin L_{II}

To determine whether nuclear lamin isoforms other than L_{III} are components of *Xenopus* oocyte nuclear envelopes, we tested a number of antilamin antibodies by immunoblotting oocyte nuclear envelope proteins separated by two-dimensional gel electrophoresis (Fig. 1). The mAb X223 (Fig. 1 *B*), previously shown to react with the B-type lamin L_{II} in *Xenopus* somatic cells (16), recognized a polypeptide of a more acidic isoelectric point than lamin L_{III} as detected by the mAb 46F7 (Fig. 1 *A*). This is demonstrated in Fig. 1 *C*, in which the 46F7 antibody-probed filter shown in Fig. 1 *A* was reprobed with the X223 antibody. These results clearly demonstrate that the antigen recognized by the X223 antibody is biochemically distinct from lamin L_{III}. Results essentially identical to Fig. 1 *C* were obtained when oocyte nuclear envelope proteins were probed with the mAb X155, which recognizes both lamins L_{II} and L_{III} (Fig. 1 *D*). In parallel experiments with lamin L_I-specific polyclonal antibodies and antilamin A-specific mAbs, we have been unable to detect these *Xenopus* lamin isoforms in isolated oocyte nuclear envelopes (data not shown).

We compared the oocyte nuclear envelope protein recognized by the antibody X223 with lamin L_{II} of ovarian follicle cells (Fig. 1 *E*) and noted that the X223-reactive protein of oocyte nuclear envelopes and lamin L_{II} of somatic cells are biochemically similar, if not identical.

The X223 antigen of oocyte nuclear envelopes has the biochemical characteristics typical of nuclear lamin proteins, including resistance to extraction with buffers containing high concentrations of monovalent salt (i.e., samples in Fig. 1) and nonionic detergents (2% Triton X-100).

To exclude the possibility that the X223 antigen in oocyte nuclear envelopes was a modified form of lamin L_{III} not recognized by the mAb 46F7, we performed in vitro translation of oocyte RNA and immunoprecipitated the products with mAbs 46F7 and X223. The primary translation products recognized by these mAbs exhibited different mobilities in gel analysis, indicating that the antigens of the 46F7 and X223 antibodies are located on separate proteins. From these results we have concluded that the protein present in nuclear envelopes of *Xenopus* oocytes is a lamin isoform identical with lamin L_{II} of somatic cells, or a very closely related lamin isotype.

Assuming equal binding affinities of the antibody X155 for lamins L_{II} and L_{III}, the quantitation of the relative amounts of lamin L_{II} to lamin L_{III} by immunoblotting of polypeptides separated by two-dimensional (Fig. 1, *D* and *C*) and one-dimensional gel electrophoresis (see Fig. 6 *C*, lane *1*) indicates that lamin L_{II} protein is ~5–10% the amount of lamin L_{III} protein observed in oocyte nuclear envelopes.

We confirmed our biochemical localization of lamin L_{II} in oocyte nuclear envelopes by immunofluorescence microscopy on cryosectioned ovarian tissue with mAbs 46F7 and X223 (Fig. 2). As expected, the antilamin L_{III} antibody 46F7 (Fig. 2 *A*) stained nuclear envelopes of oocytes, but not follicle cell nuclei. In contrast, the antilamin L_{II} antibody X223 exhibited strong staining of both oocyte nuclear envelopes and nuclei of surrounding follicle cells (Fig. 2 *B*). These results excluded the possibility that lamin L_{II} observed in the biochemical analysis of oocyte nuclear envelopes was due to follicle cell contamination of oocyte nuclei preparations.

EM immunolocalization of the X223 antigen on isolated oocyte nuclear envelopes (Fig. 3) clearly demonstrated its exclusive localization on the nucleoplasmic side of the nuclear envelope and an absence from pore complexes. These are characteristic features of nuclear lamin proteins.

Lamin L_{II} Is Present in Nuclei of Early Embryos

To determine if lamin L_{II} observed in oocyte nuclear envelopes and unfertilized egg extracts is used in the formation of daughter nuclei during early embryonic development, we performed in vitro fertilization and immunofluorescence analysis of squashed preparations of early embryos (Fig. 4). Our results demonstrate that lamins L_{III} (Fig. 4 *A*) and L_{II} (Fig. 4 *B*) are clearly visible in nuclei of 2-cell and later division embryos up to at least the 64-cell stage (data not shown). These results indicate that oocyte lamin L_{II} persists through meiotic egg maturation and is used in the formation of early embryonic nuclei.

Identification of Membrane-bound Lamins in Meiotic Egg Extracts

To verify that the *Xenopus* B-type lamin L_{II} is associated with membrane vesicles in meiotic eggs, we fractionated cytoplasm derived from meiotic eggs by high-speed centrifugation. All subfractions had been controlled for the presence of lamins by immunoblotting, and a 100,000-*g* supernatant (S_{100} *Sup.*; see Fig. 5 *A* and lane *1* in Fig. 6, *C* and *D*) appeared to contain essentially all lamins L_{II} and L_{III} of unfertilized eggs. The S_{100} Sup. contained soluble proteins and vesicles of various sizes and morphologies (Fig. 5 *A*), whereas mitochondria were relatively rare. The S_{100} Sup. was further subfractionated by centrifugation at 200,000 *g* into a membrane-enriched pellet (S_{200} *Pellet*) and a cyto-

1. *Abbreviations used in this paper*: Sup., Supernatant; TBST, Tris-buffered saline/0.3% Tween.

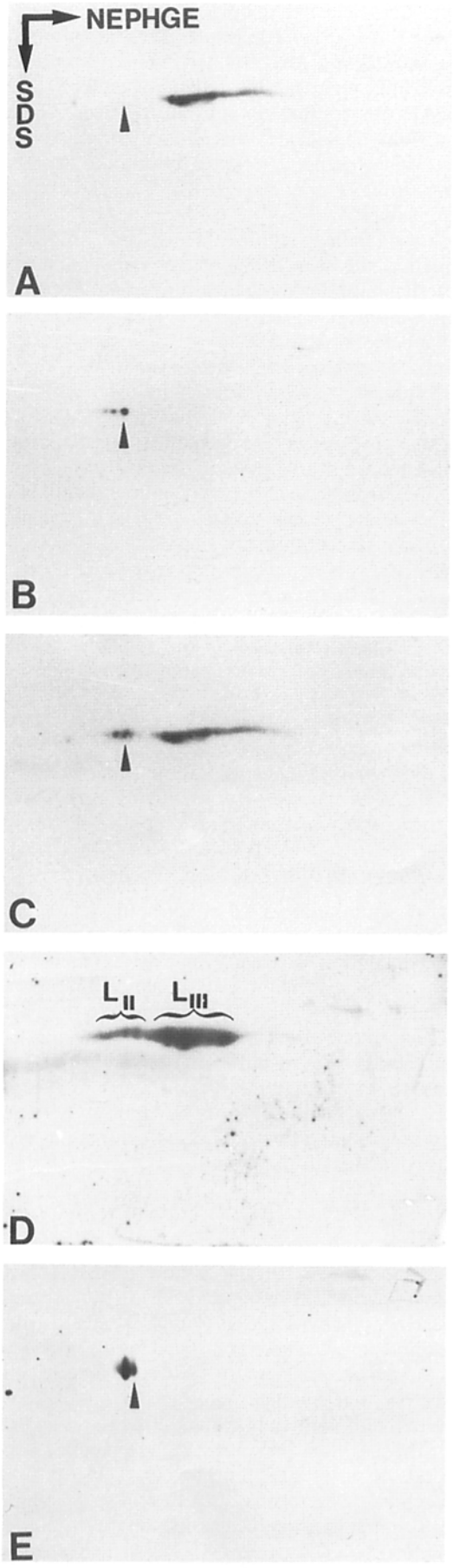

solic supernatant (*S_{200} Cytosol*). EM analysis of these fractions revealed that the S_{200} Cytosol appeared virtually free of vesicles (Fig. 5 *B*). The granular irregularly shaped material seen in the S_{200} Cytosol represents soluble proteins that had been cross-linked during gluteraldehyde fixation, resulting in the formation of large insoluble protein aggregates. In contrast, the S_{200} Pellet (Fig. 5 *C*), like the S_{100} Sup., contained vesicles of various sizes and morphologies, some of which appeared to be coated with protein aggregates resembling ribosomes.

As further controls for the separation of soluble from membrane-associated proteins in the S_{200} Cytosol and S_{200} Pellet egg-extract fractions, we immunoblotted these fractions with antibodies directed against nonlamin nuclear envelope proteins. The immunoblots of the starting material used for the generation of the S_{200} Cytosol and pellet fractions, the S_{100} Sup., are shown in lane *1* of Fig. 6, *A–D*. The nuclear pore complex protein gp62, which has previously been demonstrated to be soluble in meiotic extracts of *Xenopus* eggs (9), was present exclusively in the S_{200} Cytosol (Fig. 6 *A*, lanes *2–5*), but not detectable in the S_{200} Pellet, even when 10 times the quantity of S_{200} Pellet (Fig. 6 *A*, lane *6*) relative to S_{200} Cytosol (Fig. 6 *A*, lane *2*) was used for gel separation. In contrast, the transmembrane nuclear envelope protein p54, which has been localized to the inner nuclear membrane of chicken cells (1), was detected exclusively in the S_{200} Pellet (Fig. 6 *B*, lanes *6–8*). The membraneous nature of the material in the S_{200} Pellet was confirmed by extraction with nonionic detergent (2% Triton X-100), which solubilized essentially all proteins in the fraction including lamins L_{II} and L_{III} (data not shown). Taken together with the EM analysis shown in Fig. 5, our data demonstrate that fractionation by centrifugation at 200,000 *g* results in the clear separation of soluble from membrane-associated proteins into the S_{200} Cytosol and S_{200} Pellet fractions, respectively.

These fractions were subsequently used for the quantitation of soluble to membrane-associated lamins by immunoblot analysis with mAbs X155 (Fig. 6 *C*), which recognizes lamins L_{II} and L_{III}, and 46F7 (Fig. 6 *D*), which is specific for lamin L_{III}. In contrast to the situation in interphase cells, lamins L_{II} and L_{III} in meiotic cells exhibit different mobilities in one-dimensional gel electrophoresis. Consequently, we have been able to analyze both lamins simultaneously with the antibody X155 (Fig. 6 *C*). To enable the rela-

Figure 1. Identification of *Xenopus* lamin L_{II} in oocyte nuclear envelopes. Nuclear envelopes from 50 oocytes (*A–D*), or follicle cells derived from 25 oocytes (*E*) were salt washed and proteins electrophoretically separated by two-dimensional gel electrophoresis (first dimension, NEPHGE; second dimension, SDS-PAGE). Proteins were transferred to nitrocellulose filters and stained with Ponceau S to determine the position of the coelectrophoresed marker proteins actin, BSA, and PGK. The filters were probed with the antilamin L_{III} antibody 46F7 (*A*), the antilamin L_{II} antibody X223 (*B* and *E*), or the antilamin L_{II}/L_{III} antibody X155 (*D*). The filter shown in *A* was reprobed with the antilamin L_{II} antibody X223 (*C*). Arrowheads (*A–C* and *F*) mark the position of the quantitatively major isoelectric variant of oocyte lamin L_{II}. Brackets (*D*), indicate the isoelectric variants of L_{II} and L_{III} recognized by the antibody X155.

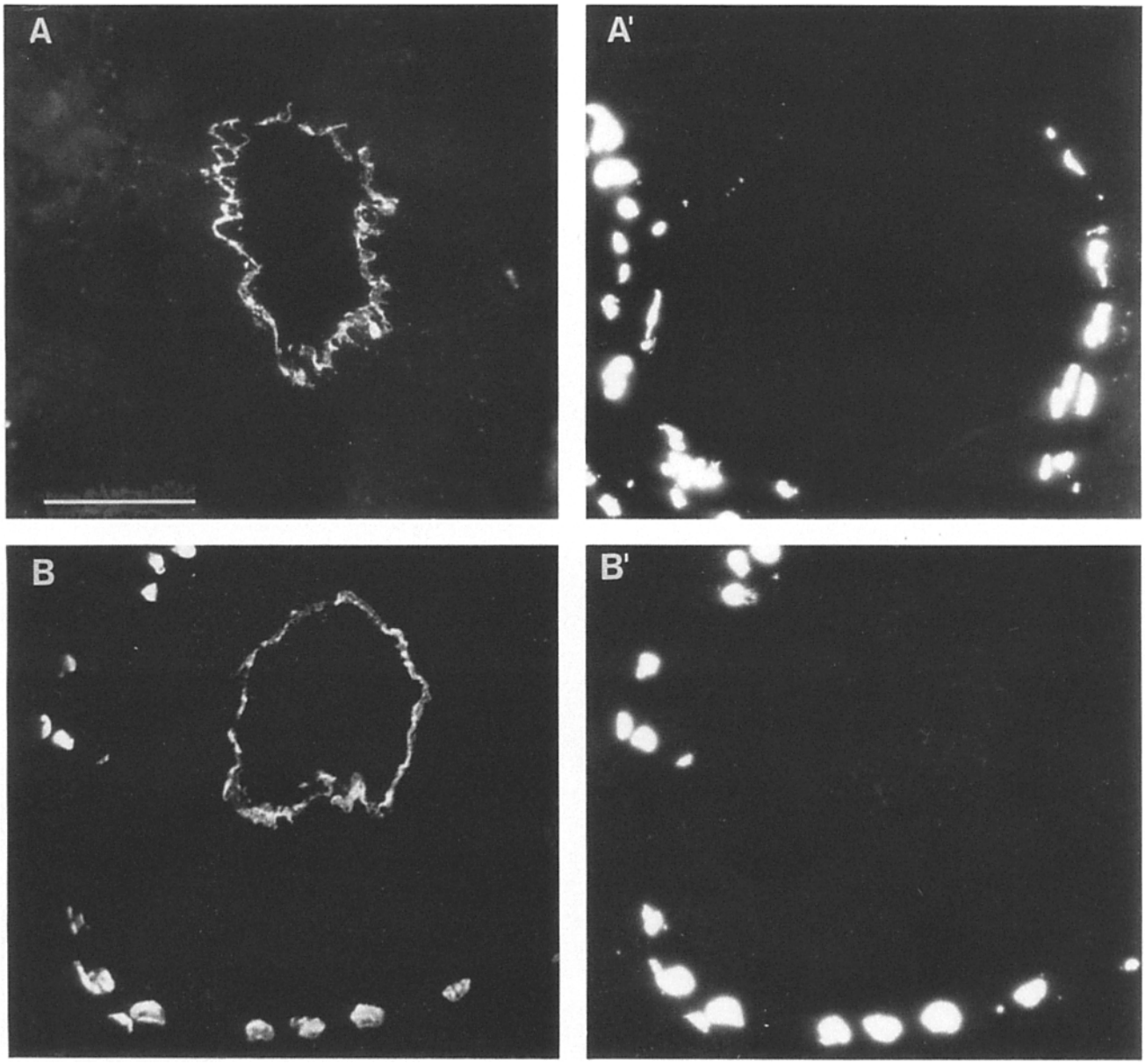

Figure 2. Immunolocalization of lamin L_{II} in ovary. Indirect immunofluorescence microscopy on *Xenopus* ovary sections after incubation with antilamin L_{III} antibody 46F7 (*A*) or antilamin L_{II} antibody X223 (*B*). Chromatin staining (*A'*, *B'*) by HOECHST. Bar, 50 μm.

tive quantitation of lamins present in both fractions, serial dilutions of S_{200} Cytosol (1.0–0.125 U; lanes *2–5*) and S_{200} Pellet (10.0–2.5 U; lanes *6–8*) were used for immunoblot analysis. One unit equals the amount of material derived from 2.4 μl of S_{100} Sup. (Fig. 6, *A–D*, lane *1*).

Immunoblotting of gel-electrophoretically separated polypeptides of both fractions with the antibody X155 (Fig. 6 *C*) demonstrated that lamins L_{II} and L_{III} were present in the membrane-free S_{200} Cytosol (lanes *2–5*), as well as in the S_{200} Pellet (lanes *6–8*). Identical results for lamin L_{III} were obtained with the antilamin L_{III} antibody 46F7 (Fig. 6 *D*). Quantitation of multiple sets of x-ray film blotting signals indicated that 20–23% of lamin L_{II} and 5–7% of lamin L_{III} were present in a membrane-associated form (Fig. 6, *C* and *D*, *S_{200} Pellet*, lanes *6–8*), whereas 77–80% of lamin L_{II} and 93–95% of lamin L_{III} were reproducibly observed in the S_{200} Cytosol fraction (lanes *2–5*).

Characterization of Lamin-associated Vesicles

For the detailed characterization of lamin-associated vesicles in meiotic egg extracts, soluble and vesicle-associated lamins in the S_{100} Sup. were immunoabsorbed to magnetic beads coated with the antilamin L_{II} antibody X223, the antilamin L_{III} antibody 46F7, or as a control, with goat anti-mouse antibodies (Fig. 7). EM analysis revealed that control magnetic beads (Fig. 7 *A*) were of various diameters and possessed an electron-dense outer surface, which was generally free of absorbed membrane material. In contrast, the antilamin L_{II}-coated beads (Fig. 7 *B*) were associated

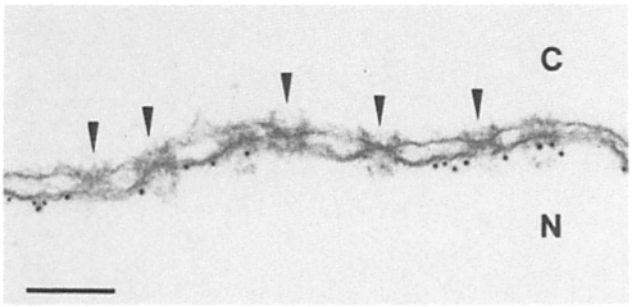

Figure 3. EM immunolocalization of lamin L_{II} to the oocyte nuclear lamina. Isolated oocyte nuclear envelopes were incubated with antilamin L_{II} antibody X223 followed by secondary antibodies conjugated to 10-nm colloidal gold. Gold particles are observed exclusively on the nucleoplasmic (*N*) side of the envelope. Nuclear pore complexes are marked by arrowheads. *C*, cytoplasmic side. Bar, 0.2 μm.

with membranes that appeared to be, within limits, rather heterogenous in size and morphology, ranging between 90 and 300 nm in diameter. On their outer surfaces, these vesicles were free of particulate material resembling ribosomes. Internally, these vesicles were not uniformly stained, although some internal structures and fibrous material appeared to be present.

To our surprise the antilamin L_{III} antibody beads incubated in S_{100} Sup. (Fig. 7, *C* and *D*) were coated with vesicles highly homogenous in size and morphology, with diameters between 40 and 80 nm. These vesicles appeared specifically on the antilamin L_{III} beads and were not observed on the control- (Fig. 7 *A*) or antilamin L_{II} (Fig. 7 *B*)-coated magnetic beads. In addition, a small number of vesicles similar in size to the antilamin L_{II}-absorbed vesicles were visible on the antilamin L_{III}-coated beads. Higher magnification images of the 40–80-nm vesicles (Fig. 7 *D*) revealed that these vesicles were similar to the lamin L_{II}-

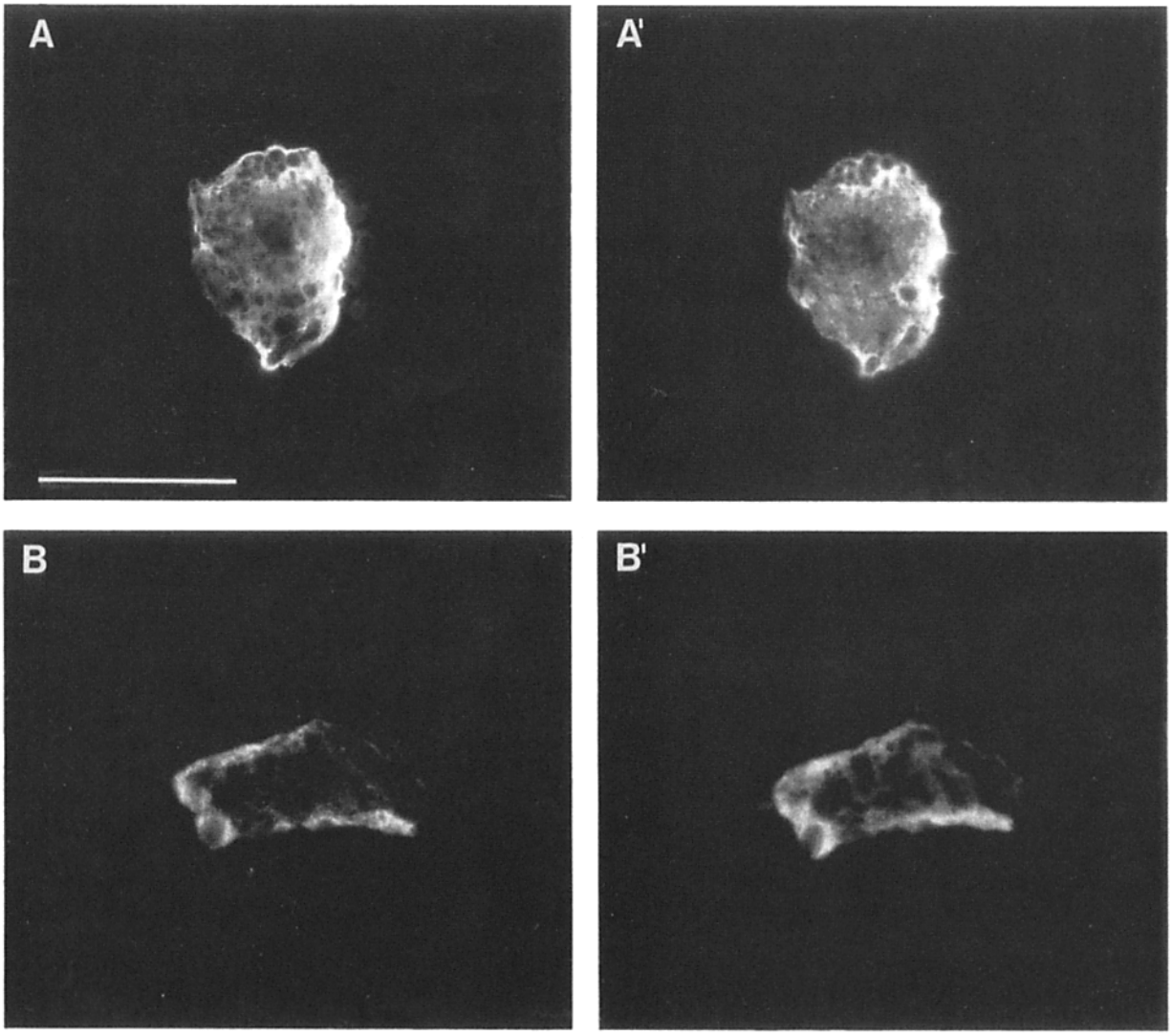

Figure 4. Immunolocalization of lamins in two-cell-stage embryos by indirect immunofluorescence microscopy. Squashed preparations of in vitro fertilized embryos halted in interphase at the two-cell stage by cycloheximide were incubated with antilamin L_{III} antibody 46F7 (*A*) or antilamin L_{II} antibody X223 (*B*), followed by Texas red-conjugated secondary antibodies. Chromatin staining (*A'* and *B'*) by HOECHST. Bar, 50 μm.

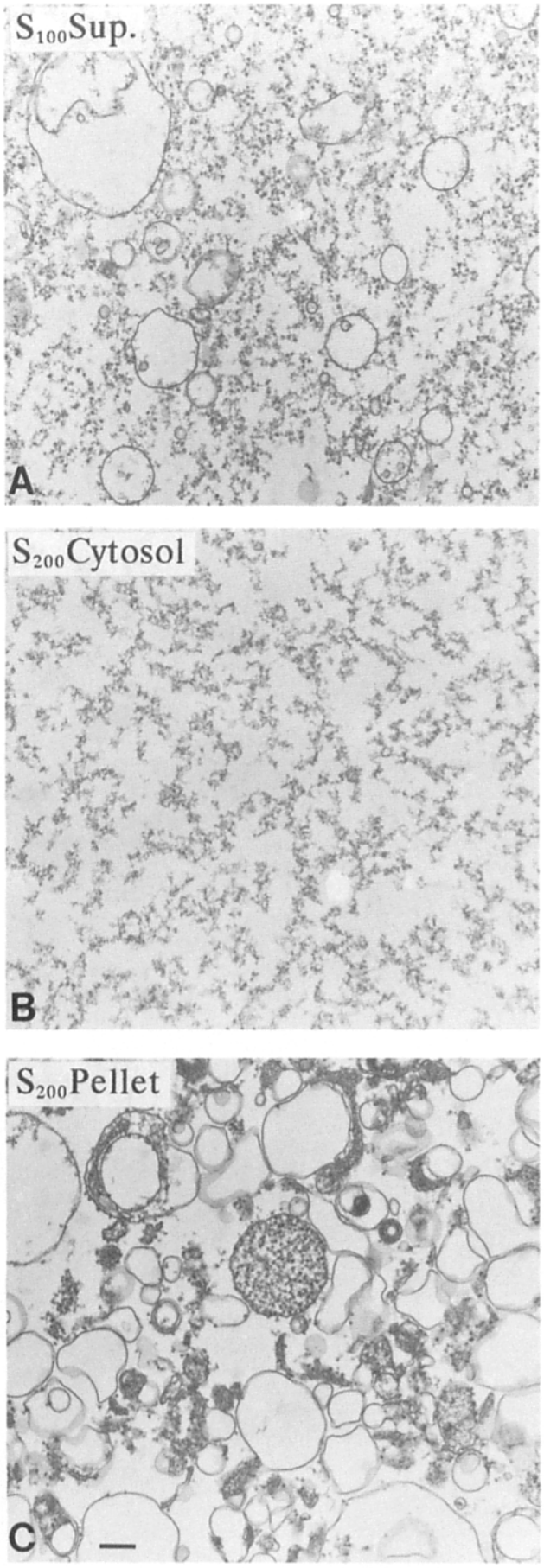

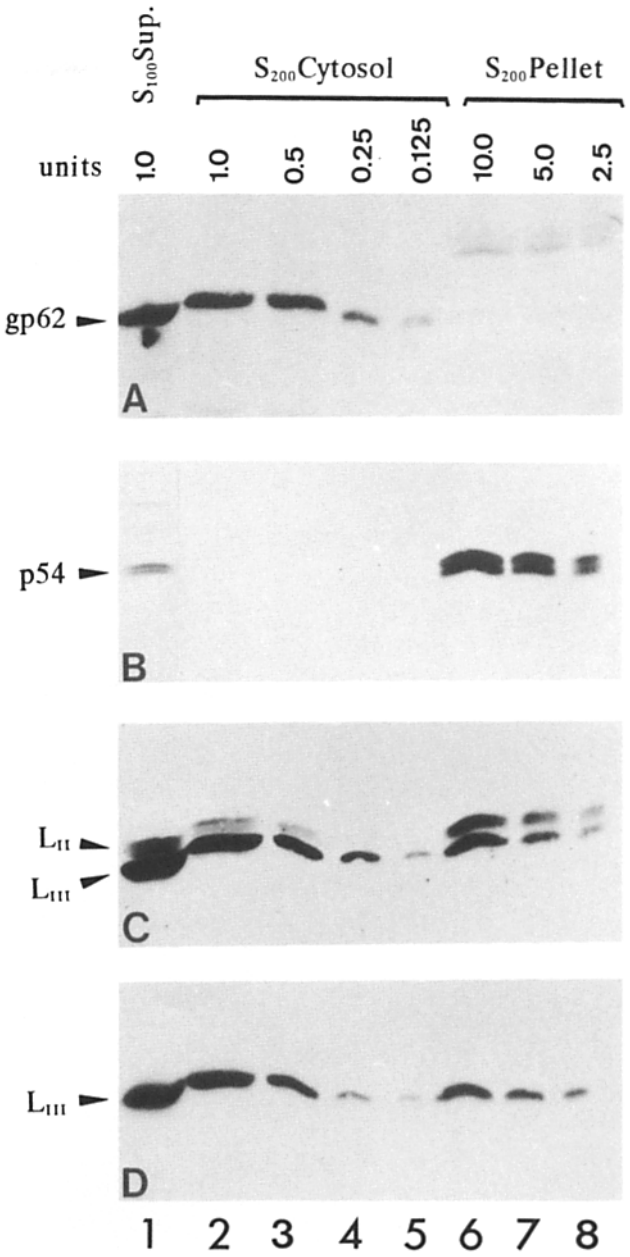

Figure 6. Distribution of nuclear envelope proteins in egg extract fractionated by ultracentrifugation. Proteins from the S_{100} Sup. (lane *1*), serial dilutions of S_{200} Cytosol (lanes *2–5*), and S_{200} Pellet (lanes *6–8*) were separated by 11% SDS-PAGE. Proteins were transferred to nitrocellulose filters then probed with anti-gp62 antiserum (*A*), anti-p54 antiserum (*B*), antilamin L_{II}/L_{III} antibody X155 (*C*), and antilamin L_{III} antibody 46F7 (*D*). Units refers to the relative amount of S_{100} Sup. (1.0 U equals 2.4 μl of S_{100} Sup., lane *1*) contained in the S_{200} Cytosol (lanes *2–5*) and S_{200} Pellet (lanes *6–8*) aliquots used for gel separation.

Figure 5. EM analysis of egg extract fractionated by ultracentrifugation. Representative examples of materials found in the S_{100} Sup. (*A*), S_{200} Cytosol (*B*), and S_{200} Pellet (*C*) are shown. Bar, 0.2 μm.

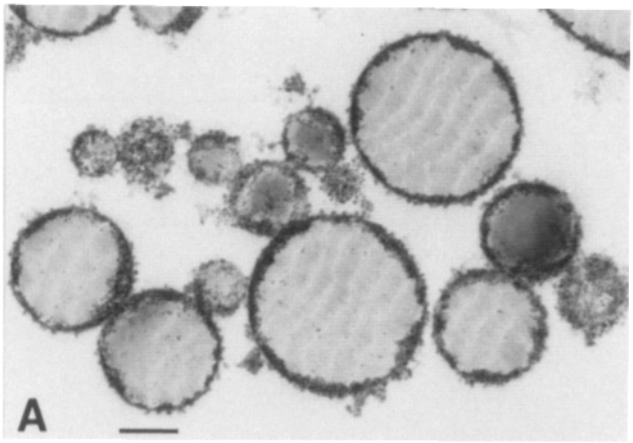

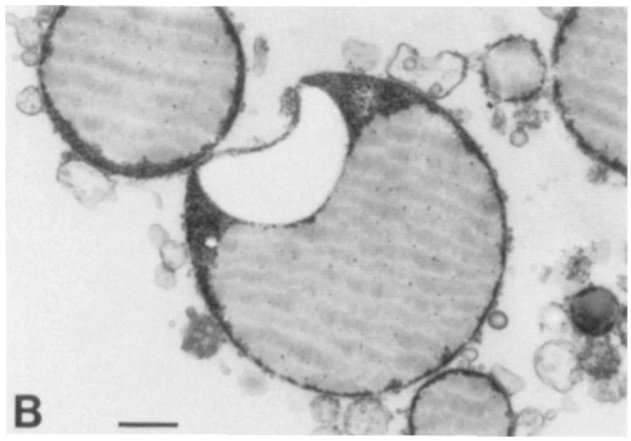

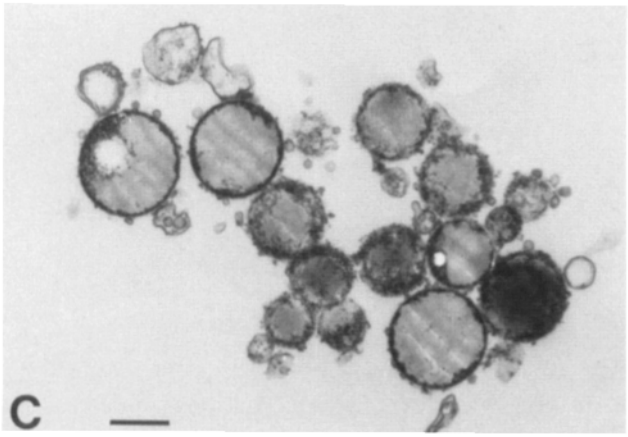

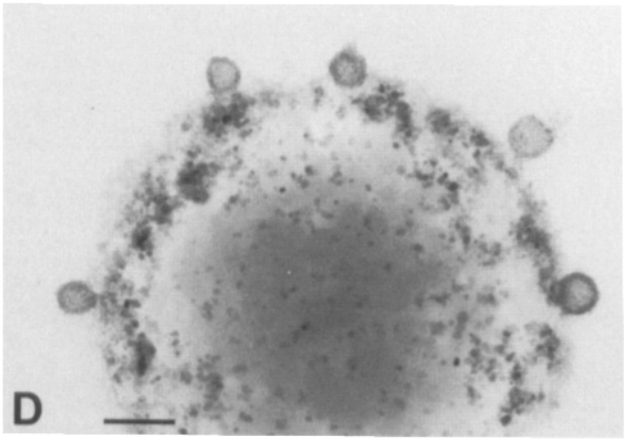

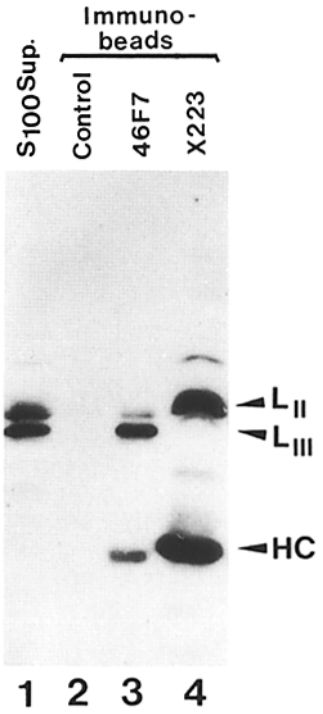

Figure 8. Immunological analysis of lamins absorbed to antibody-coated magnetic beads. An aliquot of S_{100} Sup.- (lane *1*) and proteins absorbed to control (lane *2*)-, antilamin L_{III} antibody 46F7 (lane *3*)-, and antilamin L_{II} antibody X223 (lane *4*)-coated magnetic beads were solubilized, separated by 8% SDS-PAGE, then transferred to nitrocellulose filters for probing with the antilamin L_{II}/L_{III} antibody X155. Arrowheads indicate the migration position of the antibody heavy chains (*HC*) and lamins L_{III} and L_{II} are noted on the right of the panel.

coated beads (Fig. 7 *B*) in that no particulate material resembling ribosomes appeared associated with their outer surfaces, although we could not detect any distinct stainable materials internally. We obtained similar results with antibody-coated magnetic beads incubated in the S_{200} Pellet fraction (data not shown), although a considerable amount of membranes appeared to be nonspecifically absorbed, possibly because of agglutination of membranes by centrifugation pelletting.

To biochemically characterize materials absorbed to the antibody-coated magnetic beads, proteins of the samples shown in Fig. 7, *A–D*, were separated by gel electrophoresis and analyzed by blotting with the antilamin L_{II}/L_{III} mAb X155 (Fig. 8). Lamin proteins were absent from control beads (Fig. 8, lane *2*). The antilamin L_{III}–coated beads contained large amounts of lamin L_{III} and a lesser, though significant amount of lamin L_{II} (Fig. 8, lane *3*). The presence of lamin L_{II} in this sample is consistent with the EM data (see Fig. 7 *C*), in which some membranes absorbed to antilamin L_{III}–coated beads were similar in size and morphology to vesicles absorbed to antilamin L_{II}–coated beads. Proteins absorbed to the antilamin L_{II}–coated beads included lamin L_{II} (Fig. 8, lane *4*) and did not contain detectable amounts of lamin L_{III}. In addition, we noted a protein band recognized by the antibody X155 in the antilamin L_{II} bead sample (Fig. 8, lane *4*), which had a lower mobility than lamin L_{II} in one-dimensional gel analysis. This band is

Figure 7. Immunoabsorption of vesicles to magnetic beads coated with antilamin antibodies. EM analysis of vesicles from S_{100} Sup. immunoabsorbed to magnetic beads coated with control goat anti-mouse antibody (*A*), antilamin L_{II} antibody X223 (*B*), or antilamin L_{III} antibody 46F7 (*C*; *D*, higher magnification image of 46F7-absorbed vesicles). Bars, 0.2 μm (*A–C*); 0.1 μm (*D*).

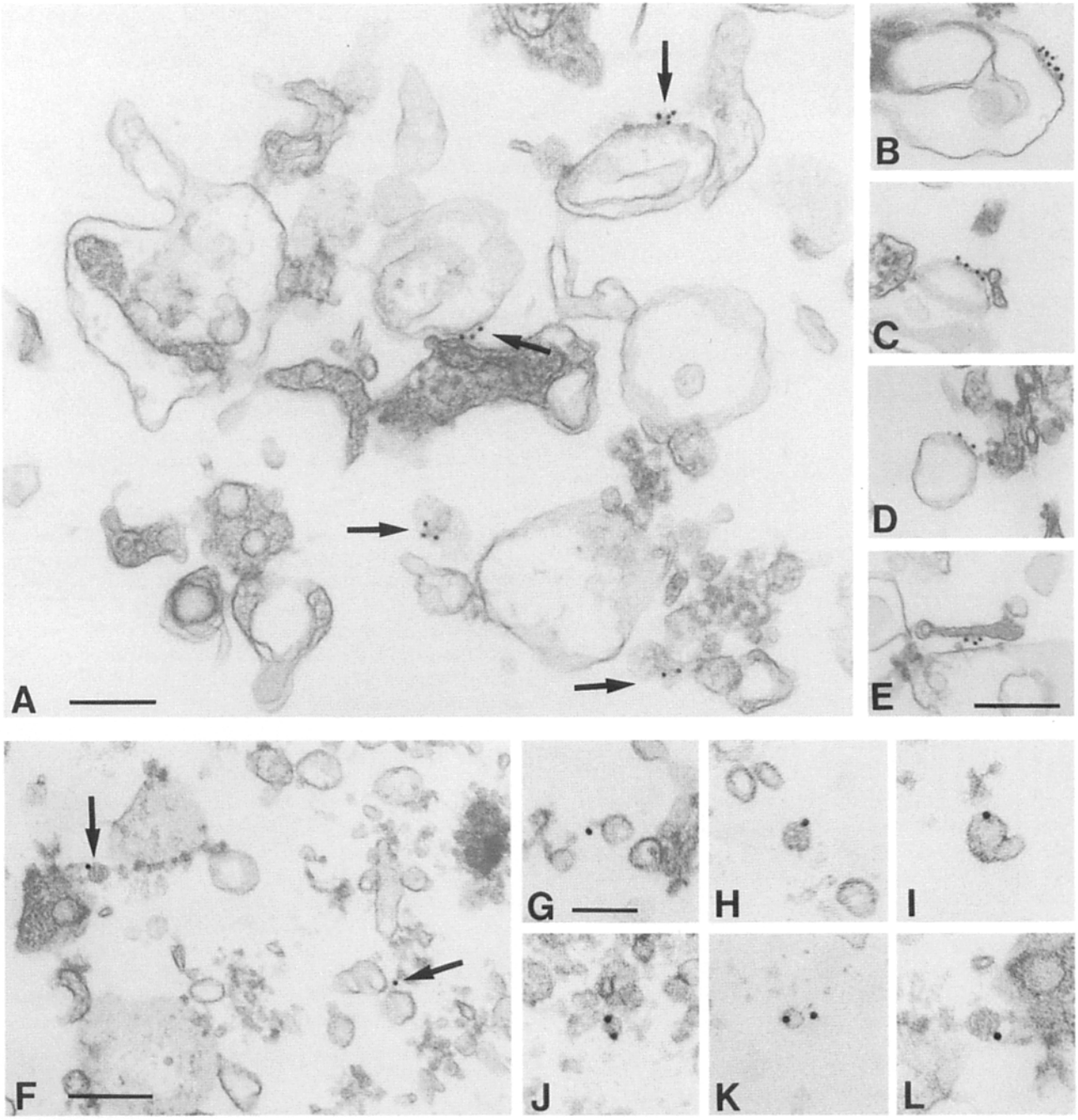

Figure 9. EM immunolocalization of lamins L_{II} and L_{III} on membranes present in the S_{200} Pellet. Membranes were immobilized onto glass coverslips and incubated with the antibodies X223 (*A–E*) or 46F7 (*F–L*). Bound antibodies were visualized with secondary antibodies conjugated to 12-nm colloidal gold. Overviews *A* (X223) and *F* (46F7) are shown at identical magnifications. Arrows in the overviews (*A* and *F*) designate vesicles labeled with gold particles. Higher magnification images of antibody X223-labeled vesicles (*B–E*) and 46F7-labeled vesicles (*G–L*) are also presented. Bars, 0.2 μm (*A* and *F*); 0.1 μm (*B–E* and *G–L*).

only faintly visible in the nonabsorbed S_{100} Sup. (Fig. 8, lane *1*), suggesting a specific enrichment of this protein with the antilamin L_{II} magnetic beads. The identity of this band is presently unknown.

In parallel to the immunoabsorption experiments, we performed immunogold localization on immobilized S_{200} Pellet membranes with the antibodies X223 (Fig. 9, *A–E*) and 46F7 (Fig. 9, *F–L*). Results obtained with this method were consistent with the immunoabsorption data (compare Figs. 7 and 9). Lamin L_{II} appeared associated with a specific subset of membranes (Fig. 9, *A–E*, see *arrows* in *A*). X223-labeled vesicles appeared to be heterogenous in size and morphology, ranging from 90 to 300 nm in diameter, and were generally free of particulate material resembling ribosomes on their outer surfaces (Fig. 9, *A–E*). The number of gold particles per labeled membrane ranged from one to five, with larger numbers of particles occasionally observed. Interestingly, the gold particles were not evenly dispersed on

the labeled membranes, but rather appeared to be clustered in a small area of the outer surface. We do not know if this nonrandom surface distribution reflects a native clustering of lamin L_{II} on membranes, or alternatively, is due to antibody–lamin L_{II} cross-linking.

Immunolocalizations on membranes of the S_{200} Pellet performed with the antilamin L_{III} antibody 46F7 revealed a specific, although sparse, gold particle labeling of membranes (Fig. 9 *F*). Labeled membranes contained one to two gold particles per vesicle and ranged in diameter from 40 to 80 nm, with no labeling of larger vesicles observed (Fig. 9, *F–L*). We have been unable to discern any internal structure within these vesicles; the outer surface appeared free of particulate material resembling ribosomes, although amorphous material was occasionally associated (see Figs. 7 *D* and 9, *F–L*).

Discussion

We have unequivocally demonstrated that, in addition to lamin L_{III}, the *Xenopus* B-type lamin L_{II} is present in oocyte nuclear envelopes. A portion of this is associated with membrane vesicles of meiotic eggs and is used for the formation of nuclei in early embryos. In addition, we have identified two separate populations of meiotic egg vesicles associated with lamins L_{II} and L_{III}, respectively. Our results indicate that the lamin composition of the amphibian oocyte and early embryo resembles the situation in birds and mammals and is more complex than previously suggested.

Why Had Previous Analysis of Xenopus Oocytes and Early Embryos Not Detected Lamin L_{II}?

We can only suggest possible factors involved in previous failures to detect lamin L_{II} in oocytes and early embryos. Immunofluorescence detection of lamin L_{II} may have been hindered by protein interactions resulting in the masking of epitopes on lamin L_{II}. Furthermore, the minor quantity of lamin L_{II} present in oocytes relative to lamin L_{III}, and their similar biochemical properties, may have made detection of lamin L_{II} difficult with the use of antibodies with a low affinity for lamin L_{II}. With this in mind, we have probed oocyte nuclear envelopes with antibody PKB8, which was previously used to screen for somatic cell lamin isoforms in oocytes (22). In immunofluorescence experiments, the antibody PKB8 does not stain the nuclear envelope of oocytes; in immunoblot experiments, only a very faint lamin L_{II} band was detected, even with use of the highly sensitive enhanced chemiluminescence antibody detection system. We suggest that the affinity of antibody PKB8 to lamin L_{II} is low and/or its lamin L_{II} epitope is not accessible in oocyte nuclear envelopes.

An alternative explanation is that the lamin L_{II} isoform recognized by the antibody X223 is an isovariant not recognized by other lamin L_{II} antibodies. Reports of alternatively spliced lamin mRNAs generating different isoforms in various species (11, 12) would support this explanation. However, we have used two separate antilamin L_{II} mAbs, X223 and X155, which recognized lamin L_{II} of oocyte nuclear envelopes and somatic cells, indicating that lamin L_{II} of both cell types contains common epitopes.

Our ability to detect lamin L_{II} in these samples may be attributed to newly available antilamin L_{II} antibodies, which recognize lamin L_{II} with high affinity at epitopes uninhibited by molecular interactions, as well as use of the highly sensitive enhanced chemiluminescence antibody detection system.

Lamin Associations with Meiotic Egg Vesicles

We and others have previously reported that lamin L_{III} appeared completely soluble in egg extracts (5, 21, 36, 49). However, in our most recent experiments, when the distribution of lamin L_{III} of unfertilized eggs was investigated by centrifugation and immunoblotting, we observed that 5–7% of the total egg lamin L_{III} was recovered in the S_{200} Pellet. Moreover, when we had diluted the S_{100} Sup. sixfold with MEB buffer containing 250 mM sucrose and centrifuged the sample at 100,000 *g*, the lamin L_{II}–associated vesicles were pelleted, but not lamin L_{III}–associated vesicles (Lourim, D., and G. Krohne, unpublished results). Our data clearly indicate that the 40–80-nm vesicles associated with lamin L_{III} are pelletable only by high speed centrifugation in low viscosity solutions, suggesting a possible explanation why lamin L_{III}–associated vesicles had not previously been detected. Furthermore, our ability to separate the lamin L_{II}–associated membranes from L_{III}–associated membranes supports the suggestion that lamins L_{II} and L_{III} are bound to separate vesicle populations.

We have reproducibly detected lamin L_{II} absorbed to beads coated with the antilamin L_{III} antibody 46F7 (Fig. 8, lane *6*). We can dismiss the possibility that this result was caused by cross-reactivity of the antilamin L_{III} antibody 46F7 with lamin L_{II}, for, when immunoprecipitations with this antibody were performed in the presence of nonionic detergents, lamin L_{III} was exclusively absorbed to antilamin L_{III} immunobeads. Furthermore, this coabsorption cannot be explained by the suggestion of a population of vesicles that possess both lamins L_{II} and L_{III}, because we have not detected significant amounts of lamin L_{III} absorbed to the lamin L_{II}–specific antibody X223–coated beads (compare Fig. 8, lanes *6* and *7*). In addition, vesicle fusion was inhibited under our experimental conditions by the inclusion of the membrane fusion inhibitor GTPγS, the phosphatase inhibitor β-glycerophosphate, and ATP to maintain protein phosphorylation. Further experiments are required to clarify this result.

The Relationship of Lamin-associated Vesicles to the Nuclear Envelope-Precursor Membranes As Described by Others

The *Xenopus* meiotic egg vesicles associated with lamin L_{II} we have described here are, on average, between 90 and 300 nm in diameter. These vesicles appear to be similar in size and heterogeneity to the lamin B–associated vesicles immunoabsorbed from mitotic CHO cell-free extracts (100–300 nm diam, as measured from micrographs presented in reference 6), but are clearly different in size and morphology from two previously described membrane populations (500–700 nm diam) of *Xenopus* egg extracts containing nuclear envelope–forming activities (48, 49). It is unlikely that these differences in *Xenopus* meiotic egg vesicle sizes are due to fusion of our membranes during preparation, because we have included membrane fusion and phosphatase inhibitors in all isolation and wash buffers (see above and Materials and

Methods). However, these differences in vesicle sizes may be due to physiological differences between extracts of activated (35, 48) and nonactivated (our results) eggs.

Interestingly, the 70–80-nm vesicles of *Xenopus* egg extracts that exhibit chromatin-binding activity as described by Newport and Dunphy (35) appear to be similar in size and morphology to vesicles we have observed bound to antilamin L_{III} immunobeads (Fig. 7, *C* and *D*). However, our membrane preparations contained a large number of vesicles in the size range of 40–80 nm, with a very small subset of these vesicles being labeled by the antilamin L_{III} antibody (Fig. 9, *F–L*). Whether or not the chromatin-binding vesicles previously described (35, 52) contain lamin isoforms has yet to be determined. Moreover, as the ability of lamin L_{III} to bind chromatin has not been established, the proteins responsible for vesicle–chromatin interaction need to be determined.

The Potential Role of B-Type Lamin-associated Membranes in Nuclear Envelope Re-formation After Meiosis and Mitosis

In nuclear reconstitution experiments, Newport et al. (36) observed that nuclear envelopes formed around demembranated *Xenopus* sperm from *Xenopus* extracts that had been depleted of lamin L_{III} with the antibody 46F7 (from our laboratory) and concluded that there must be a lamin-independent pathway involved in the initial phases of nuclear envelope assembly. However, for these experiments, a membrane-free fraction of egg extracts had been immunodepleted. In contrast, using complete *Xenopus* egg extracts immunodepleted with the antilamin L_{III} antibody S49H2 (from our laboratory), Dabauvalle et al. (10) reported an inhibition of nuclear envelope formation around bacteriophage DNA, but no inhibition in the formation of cytoplasmic annulate lamellae. The resolution of the apparent contradiction between the results of Dabauvalle et al. (10), and Newport et al. (36) may lie in the observations noted above, and in our recent determination that the antibody S49H2 recognizes lamin L_{II} as well as lamin L_{III} (Lourim, D., and G. Krohne, unpublished observations). Consequently, regarding the experiments of Dabauvalle et al. (10), we suggest that incubation of whole-egg extracts with S49H2 had inhibited or depleted the chromatin-binding activity of lamins L_{II} and L_{III}. Taken together, these results indicate that membrane-associated lamins may be involved in the targeting of nuclear envelope precursor vesicles to chromatin substrates after mitosis and meiosis. Moreover, nuclear reconstitution experiments performed with cell-free extracts of mammalian tissue culture cells (6) and *Drosophila* embryos (47) have shown that lamins are involved in nuclear envelope re-formation after mitosis in these systems.

Our results for *Xenopus* eggs suggest that lamin associations with vesicles of meiotic eggs may differ in some respects from the situation in mitotic somatic cells. There are no indications of a population of nonmembrane-associated B-type lamins in mitotic somatic cells (6, 13, 46), whereas in egg extracts of *Xenopus* (our results), a majority (77–80% of lamin L_{II}) of B-type lamin appears not to be associated with vesicles (compare Fig. 5 *D*, lanes *3–5*, and Fig. 7, *B* and *F*). These results suggest the existence of a mechanism that limits association of B-type lamins, including lamin L_{III}, with membranes of meiotic cells.

Our description of a B-type lamin in oocyte nuclear envelopes and of membrane-associated lamins in meiotic egg extracts will help to determine the role of lamins in nuclear envelope re-formation. We are currently analyzing the potential of vesicle-associated lamins to target membranes to the surface of chromatin, as well as characterizing the abundance and protein composition of lamin-associated vesicles.

We are very grateful to Anja Schneider, Marianne Schmidt, and Hilde Merkert for their assistance, and Claudia Gehrig for electron microscope and photographic technical assistance. We thank Stefan Büchler for performing the immunofluorescence analysis of *Xenopus* embryo squashed preparations. We appreciate the gift of the anti-p54 antiserum from Erich Nigg. We would like to thank the JCB editors and reviewers for their careful readings of the manuscript, and their subsequent suggestions. We are indebted to Ulrich Scheer for support, Ricardo Benavente and Marie-Christine Dabauvalle (Biocenter, Würzburg, Germany) for helpful discussions and critical readings of the manuscript, and Lynn Leverenz for correcting the manuscript.

D. Lourim is an Alexander Von Humboldt Research Fellow. This work was supported by grant Kr 758/4-3 to G. Krohne from the Deutsche Forschunggemeinschaft.

Received for publication 11 May 1993 and in revised form 16 July 1993.

References

1. Bailer, S., H. Eppenberger, G. Griffiths, and E. Nigg. 1991. Characterization of a 54-kD protein of the inner nuclear membrane: evidence for cell cycle–dependent interaction with the nuclear lamina. *J. Cell Biol.* 114:389–400.
2. Beams, H., and S. Mueller. 1970. Effect of ultracentrifugation on the interphase nucleus of somatic cell with special reference to the nuclear envelope–chromatin relationship. *Z. Zellforsch.* 108:297–308.
3. Beck, L., T. Hosick, and M. Sinensky. 1990. Isoprenylation is required for the processing of the lamin A precursor. *J. Cell Biol.* 110:1489–1499.
4. Benavente, R., and G. Krohne. 1986. Involvement of nuclear lamins in postmitotic reorganization of chromatin as demonstrated by microinjection of lamin antibodies. *J. Cell Biol.* 103:1847–1854.
5. Benavente, R., G. Krohne, and W. Franke. 1985. Cell type–specific expression of nuclear lamina proteins during development of *Xenopus laevis*. *Cell.* 41:177–190.
6. Burke, B., and L. Gerace. 1986. A cell free system to study reassembly of the nuclear envelope at the end of mitosis. *Cell.* 44:639–652.
7. Cordes, V., I. Waizenegger, and G. Krohne. 1991. Nuclear pore complex glycoprotein p62 of *Xenopus laevis* and mouse: cDNA cloning and identification of its glycosylated region. *Eur. J. Cell Biol.* 55:31–47.
8. Dabauvalle, M.-C., and U. Scheer. 1991. Assembly of nuclear pore complexes in *Xenopus* egg extract. *Biol. Cell.* 72:25–29.
9. Dabauvalle, M.-C., K. Loos, and U. Scheer. 1990. Identification of a soluble precursor complex essential for nuclear pore assembly in vitro. *Chromosoma.* 100:56–66.
10. Dabauvalle, M.-C., K. Loos, H. Merkert, and U. Scheer. 1991. Spontaneous assembly of pore complex–containing membranes ("Annulate Lamellae") in *Xenopus* egg extract in the absence of chromatin. *J. Cell Biol.* 112:1073–1082.
11. Doring, V., and R. Stick. 1990. Gene structure of nuclear lamin L_{III} of *Xenopus laevis*: a model for the evolution of IF proteins from a lamin-like ancestor. *EMBO (Eur. Mol. Biol. Organ.) J.* 9:4073–4081.
12. Furukawa, K., and Y. Hotta. 1993. cDNA cloning of a germ cell specific lamin B_3 from mouse spermatocytes and analysis of its function by ectopic expression in somatic cells. *EMBO (Eur. Mol. Biol. Organ.) J.* 12:97–106.
13. Gerace, L., and G. Blobel. 1980. The nuclear envelope lamina is reversibly depolymerized during mitosis. *Cell.* 19:277–287.
14. Gieffers, C., and G. Krohne. 1991. In vitro reconstitution of recombinant lamin A and a lamin A mutant lacking the carboxy-terminal tail. *Eur. J. Cell Biol.* 55:191–199.
15. Glass, J., and L. Gerace. 1990. Lamins A and C bind and assemble at the surface of mitotic chromosomes. *J. Cell Biol.* 111:1047–1057.
16. Höger, T., K. Zatloukal, I. Waizenegger, and G. Krohne. 1990. Characterization of a second highly conserved B-type lamin present in cells previously thought to contain only a single B-type lamin. *Chromosoma.* 99:379–390.
17. Höger, T., C. Grund, W. Franke, and G. Krohne. 1991. Immunolocalization of lamins in the thick nuclear lamina of human synovial cells. *Eur.*

J. Cell Biol. 54:150–156.
18. Höger, T., G. Krohne, J. Kleinschmidt. 1991. Interaction of *Xenopus* lamins A and L_{II} with chromatin in vitro mediated by a sequence element in the carboxyterminal domain. *Exp. Cell Res.* 197:280–289.
19. Hutchison, C., R. Cox, and C. Ford. 1988. The control of DNA replication in a cell-free extract that recapitulates a basic cell cycle in vitro. *Development.* 103:553–566.
20. Krohne, G., and R. Benavente. 1986. The nuclear lamins: a multigene family of proteins in evolution and differentiation. *Exp. Cell Res.* 162:1–10.
21. Krohne, G., and R. Benavente. 1986. A pool of soluble nuclear lamins in eggs and embryos of *Xenopus laevis*. *In* Nucleocytoplasmic Transport. R. Peters and M. Trendelenburg, editors. Springer-Verlag, New York. 135–141.
22. Krohne, G., E. Debus, M. Osborn, K. Weber, and W. Franke. 1984. A monoclonal antibody against nuclear lamina proteins reveals cell type-specificity in *Xenopus laevis*. *Exp. Cell Res.* 150:47–59.
23. Krohne, G., S. Wolin, F. McKeon, W. Franke, and M. Kirschner. 1987. Nuclear lamin L_I of *Xenopus laevis*: cDNA cloning, amino acid sequence and binding specificity of a member of the lamin B subfamily. *EMBO (Eur. Mol. Biol. Organ.) J.* 6:3801–3808.
24. Kyhse-Andersen, J. 1984. Electroblotting of multiple gels: a simple apparatus without tank for rapid transfer of proteins from polyacrylamide to nitrocellulose. *J. Biochem. Biophys. Methods.* 10:203–210.
25. Laemmli, U. 1970. Cleavage of structural proteins during assembly of the head of the bacteriophage T4. *Nature (Lond.).* 227:680–685.
26. Laskey, R., and G. Leno. 1990. Assembly of the cell nucleus. *Trends Genet.* 6:406–410.
27. Lebel, S., C. Lampron, and Y. Raymond. 1987. Lamins A and C appear during retinoic acid–induced differentiation of mouse embryonal cells. *J. Cell Biol.* 105:1099–1104.
28. Lebkowski, J., and U. Laemmli. 1982. Non-histone proteins and long-range organization of HeLa interphase DNA. *J. Mol. Biol.* 156:325–344.
29. Lehner, C., R. Stick, H. Eppenberger, and E. Nigg. 1987. Differential expression of nuclear lamin proteins during chicken development. *J. Cell Biol.* 105:577–587.
30. Lourim, D., and J. J.-C. Lin. 1989. Expression of nuclear lamin A and muscle-specific proteins in differentiating muscle cells in ovo and in vitro. *J. Cell Biol.* 109:495–504.
31. Lourim, D., and J. J.-C. Lin. 1992. Expression of wild-type and nuclear localization–deficient human lamin A in chick myogenic cells. *J. Cell Sci.* 103:863–874.
32. Ludérus, M., A. Graaf, E. Mattia, J. Blaauwen, M. Grande, L. de Jong, and R. Driel. 1992. Binding of matrix attachment regions to lamin B_1. *Cell.* 70:949–959.
33. McKeon, F., M. Kirschner, and D. Caput. 1986. Homologies in both primary and secondary structure between nuclear envelope and intermediate filament proteins. *Nature (Lond.).* 319:463–468.
34. Meier, J., K. Campbell, C. Ford, R. Stick, and C. Hutchison. 1991. The role of lamin L_{III} in nuclear assembly and DNA replication, in cell-free extracts of *Xenopus* eggs. *J. Cell Sci.* 98:271–279.
35. Newport, J., and W. Dunphy. 1992. Characterization of the membrane binding and fusion events during nuclear envelope assembly using purified components. *J. Cell Biol.* 116:295–306.
36. Newport, J., K. Wilson, and W. Dunphy. 1990. A lamin-independent pathway for nuclear envelope assembly. *J. Cell Biol.* 111:2247–2259.
37. Nigg, E. 1989. The nuclear envelope. *Curr. Opin. Cell Biol.* 1:435–440.
38. O'Farrell, P., H. Goodman, and P. H. O'Farrell. 1977. High resolution two-dimensional electrophoresis of basic as well as acidic proteins. *Cell.* 12:1133–1142.
39. Peter, M., G. Kitten, C. Lehner, K. Vorburger, S. Bailer, G. Maridor, and E. Nigg. 1989. Cloning and sequencing of cDNA clones encoding chicken lamin A and B_1 and comparison of the primary structures of vertebrate A- and B-type lamins. *J. Mol. Biol.* 208:393–404.
40. Röber, R.-A., K. Weber, and M. Osborn. 1989. Differential timing of nuclear lamin A/C expression in the various organs of the mouse embryo and the young animal: a developmental study. *Development.* 105: 365–378.
41. Schatten, G., G. Maul, H. Schatten, N. Chaly, C. Simerly, R. Balczon, and D. Brown. 1985. Nuclear lamins and peripheral nuclear antigens during fertilization and embryogenesis in mice and sea urchins. *Proc. Natl. Acad. Sci. USA.* 82:4727–4731.
42. Stewart, C., and B. Burke. 1987. Teratocarcinoma stem cells and early mouse embryos contain only a single major lamin polypeptide closely resembling lamin B. *Cell.* 51:383–392.
43. Stick, R. 1988. cDNA cloning of the developmentally regulated lamin L_{III} of *Xenopus laevis*. *EMBO (Eur. Mol. Biol. Organ.) J.* 7:3189–3197.
44. Stick, R. 1992. The gene structure of *Xenopus* nuclear lamin A: a model for the evolution of A-type from B-type lamins by exon shuffling. *Chromosoma.* 101:566–574.
45. Stick, R., and P. Hausen. 1985. Changes in the nuclear lamina composition during early development of *Xenopus laevis*. *Cell.* 41:191–200.
46. Stick, R., B. Angres, C. Lehner, and E. Nigg. 1988. The fates of chicken nuclear lamin proteins during mitosis: evidence for a reversible redistribution of lamin B_2 between inner nuclear membrane and elements of the endoplasmic reticulum. *J. Cell Biol.* 107:397–406.
47. Ulitzur, N., A. Harel, N. Feinstein, and Y. Gruenbaum. 1992. Lamin activity is essential for nuclear envelope assembly in a *Drosophila* embryo cell-free extract. *J. Cell Biol.* 119:17–25.
48. Vigers, G. P. A., and M. Lohka. 1991. A distinct vesicle population targets membranes and pore complexes to the nuclear envelope in *Xenopus* eggs. *J. Cell Biol.* 112:545–556.
49. Vigers, G. P. A., and M. Lohka. 1992. Regulation of nuclear envelope precursor functions during cell division. *J. Cell Sci.* 102:273–284.
50. Vorburger, K., G. Kitten, and E. Nigg. 1989. Modification of nuclear lamin proteins by a mevalonic acid derivative occurs in reticulocyte lysates and requires the cystein residue of the C-terminal CXXM motif. *EMBO (Eur. Mol. Biol. Organ.) J.* 8:4007–4013.
51. Weber, K., U. Plessmann, and P. Traub. 1989. Maturation of nuclear lamin A involves a specific carboxy-terminal trimming, which removes the polyisoprenylation site from the precursor: implications for the structure of the nuclear lamina. *FEBS (Fed. Eur. Biochem. Soc.) Lett.* 257: 411–414.
52. Wilson, K., and J. Newport. 1988. A trypsin-sensitive receptor on membrane vesicles is required for nuclear envelope formation in vitro. *J. Cell Biol.* 107:57–68.
53. Wolin, S., G. Krohne, and M. Kirschner. 1987. A new lamin in *Xenopus* somatic tissues displays strong homology to human lamin A. *EMBO (Eur. Mol. Biol. Organ.) J.* 6:3809–3818.
54. Zewe, M., T. Höger, T. Fink, P. Lichter, G. Krohne, and W. Franke. 1991. Gene structure and chromosomal localization of the murine lamin B2 gene. *Eur. J. Cell Biol.* 56:342–350.